Oceanologia (2016) 58, 201–211

Available online at www.sciencedirect.com

ScienceDirect

journal homepage: www.elsevier.com/locate/oceano

ORIGINAL RESEARCH ARTICLE

Phytoplankton pigments and functional community structure in relation to environmental factors in the Pearl River Estuary☆

Chao Chai [a,b], **Tao Jiang** [b,*], **Jingyi Cen** [c], **Wei Ge** [d], **Songhui Lu** [c,**]

[a] *Qingdao Engineering Research Center for Rural Environment, Qingdao Agricultural University, Qingdao, China*
[b] *Key Laboratory of Sustainable Development of Marine Fisheries, Ministry of Agriculture, Yellow Sea Fisheries Research Institute, Chinese Academy of Fishery Sciences, Qingdao, China*
[c] *Research Center for Harmful Algae and Marine Biology, Jinan University, Guangzhou, China*
[d] *College of Life Sciences, Qingdao Agricultural University, Qingdao, China*

Received 11 April 2015; accepted 8 March 2016
Available online 31 March 2016

KEYWORDS
Phytoplankton;
Pigments;
Functional community;
HPLC;
Pearl River Estuary

Summary Two cruises were undertaken in the Pearl River Estuary in November 2011 and March 2012 to analyze the distribution of phytoplankton pigments and to define the relationships of pigment indices and functional community structure with environmental factors. Among 22 pigments, 17 were detected by high-performance liquid chromatography. Chlorophyll *a* was found in all samples, with a maximum of 7.712 $\mu g\ L^{-1}$ in spring. Fucoxanthin was the most abundant accessory pigment, with mean concentrations of 2.914 $\mu g\ L^{-1}$ and 0.207 $\mu g\ L^{-1}$ in spring and autumn, respectively. Chlorophyll *a*, chlorophyll c_2, fucoxanthin, diadinoxanthin, and diatoxanthin were high in the northern or northwest estuary in spring and in the middle-eastern and northeast estuary in autumn. Chlorophyll *b*, chlorophyll c_3, prasinoxanthin, and peridinin were similarly distributed during the two cruises. Chlorophyll *a* and fucoxanthin positively correlated with nutrients in spring, whereas 19′-hex-fucoxanthin and 19′-but-fucoxanthin

☆ Support for this study was partly provided by the projects 'National Natural Science Foundation of China (41476098), Special Scientific Research Funds for Central Non-profit Institutes, Yellow Sea Fisheries Research Institutes (20603022015002), and Open Foundation of Key Laboratory of South China Sea Fishery Resources Development and Utilization, Ministry of Agriculture (LSF2014-04)'.

* Corresponding author at: Key Laboratory of Sustainable Development of Marine Fisheries, Ministry of Agriculture, Yellow Sea Fisheries Research Institute, Chinese Academy of Fishery Sciences, Qingdao 266071, China. Tel.: +86 53285806341.
** Corresponding author at: Research Center for Harmful Algae and Marine Biology, Jinan University, Guangzhou 510632, China. Tel.: +86 2085222720.
E-mail address: jiangtaophy@163.com (T. Jiang).

Peer review under the responsibility of Institute of Oceanology of the Polish Academy of Sciences.

ELSEVIER Production and hosting by Elsevier

http://dx.doi.org/10.1016/j.oceano.2016.03.001

negatively correlated. The biomass proportion of microphytoplankton (BP_m) was higher in spring, whereas that of picophytoplankton (BP_p) was higher in autumn. BP_m in spring was high in areas with salinity <30, but BP_p and the biomass proportion of nanophytoplankton (BP_n) were high in areas with salinity >30. BP_m increased but BP_n reduced with the increase in nutrient contents. By comparison, BP_p reduced with the increase in nutrient contents in spring, but no relationship was found between BP_p and nutrient contents in autumn. The ratios of photosynthetic carotenoids to photoprotective carotenoids in the southern estuary approached unity linear relationship in spring and were under the unity line in autumn.

1. Introduction

The Pearl River Estuary (PRE) is situated in southern Guangdong Province, China, along the northern boundary of the South China Sea. It receives most of the outflow from the Pearl River, which is the third longest river in China and the 13th largest river by discharge in the world (Lerman, 1981). The Pearl River drains an area of 453,700 km^2, and some of the most densely populated cities, such as Hong Kong, Macau, Shenzhen, Zhuhai, Guangzhou, are located on the Pearl River Delta. Approximately 19 billion tons of domestic, industrial, and agricultural effluents are annually discharged to the drainage basin of the Pearl River (Bulletin of Water Resources in the Pearl River Drainage, 2011, 2012). Therefore, the PRE has been experiencing deterioration of its aquatic environment (He et al., 2014; Qiu et al., 2010).

Phytoplankton is the base of food webs and the principal source of organic production in aquatic ecosystems. The biomass, composition, and community structure of phytoplankton can serve as indices to monitor aquatic environments (Paerl et al., 2003). Meanwhile, the distribution and succession of phytoplankton are the consequences of adaption to different environmental conditions, such as temperature, discharge, nutrients, and light intensity (Margalef, 1978).

Many studies have investigated the diversity, distribution, and seasonal variation of cell abundance of phytoplankton in the PRE (Huang et al., 2004; Li et al., 2014; Yin et al., 2000, 2001, 2004). Most previous studies have employed microscopy to identify and analyze phytoplankton quantitatively in the PRE. However, this method is time consuming and requires taxonomic knowledge (Naik et al., 2011). Moreover, picophytoplankton are typically not identified or counted with the use of this method (Jeffrey et al., 1997). Alternatively, photosynthetic pigments can be easily detected and can serve as biomarkers for particular classes or even genera of phytoplankton (Wright and Jeffrey, 2006). Pigment detection based on high-performance liquid chromatography (HPLC) methods enables quantification of over 50 phytoplankton pigments (Aneeshkumar and Sujatha, 2012; Jeffrey et al., 1997). Some photosynthetic pigments (e.g., fucoxanthin, peridinin, alloxanthin, zeaxanthin, chlorophyll *b*, 19′-hex-fucoxanthin, and 19′-but-fucoxanthin) can be considered diagnostic pigments (DP) of specific phytoplankton groups (diatoms, dinoflagellates, cryptophytes, cyanobacteria, chlorophytes, haptophytes, and pelagophytes, respectively) (Barlow et al., 2008; Paerl et al., 2003). Moreover, diatoxanthin and diadinoxanthin are generally found in diatoms and dinoflagellates, whereas prasinoxanthin, lutein, violaxanthin, and neoxanthin are found in prasinophyceae and chlorophyceae. Chlorophyll *a*, *c*, and β,β-carotene are general indicators of total algal biomass. Phytoplankton cells are categorized into three groups according to their sizes (equivalent spherical diameter): microphytoplankton (20–200 μm), nanophytoplankton (2–20 μm), and picophytoplankton (0.2–2 μm) (Sieburth et al., 1978). The contribution of each group is also reflected by its pigment signatures (Vidussi et al., 2001). Therefore, photosynthetic pigment biomarkers are widely used in oceanography for quantifying phytoplankton biomass and assessing the structure of phytoplankton community (Paerl et al., 2003; Wright and Jeffrey, 2006).

Photosynthetic pigments also function as indicators of the physiological condition of a phytoplankton community, which may be affected by environmental and trophic conditions (Roy et al., 2006). Photoprotective carotenoids (PPCs) are more dominant in low productivity waters, whereas photosynthetic carotenoids (PSCs) are dominant in high productivity waters (Barlow et al., 2002; Gibb et al., 2000). In addition, intensive light increases the PPC:PSC ratio (Moreno et al., 2012; Vijayan et al., 2009). Thus, PPC:PSC ratio is considered a good indicator of environmental factors.

Estuarine environmental factors often vary markedly in spatial and temporal scales, thereby affecting phytoplankton physiology, biomass, and communities. The PRE has a complex estuarine environment in terms of freshwater input, turbidity and irradiance, nutrient content and composition, etc. However, few studies have observed the spatial and temporal distribution of phytoplankton pigments, as well as the functional community structure, in relation to environmental factors in the PRE. The present study aims to describe the spatial–temporal distribution of phytoplankton pigments in the PRE and to define the relationships of pigment indices and functional community structure with environmental factors.

2. Material and methods

2.1. Study area

The PRE is triangular and encompasses a large area of approximately 1900 km^2. It is approximately 60 km long and 10 km wide at its head and 60 km at its mouth. The PRE is shallow, with a depth of 2–10 m (Harrison et al., 2008). It has a subtropical climate with a long summer and a short winter. The Pearl River mainly consists of three branches (Xi Jiang, Bei Jiang, and Dong Jiang) with eight outlets, four of which enter the estuary (Harrison et al., 2008). Its annual average

discharge is approximately 10,000 $m^3 s^{-1}$ (Zhai et al., 2005), with 20% occurring from October to March next year (the dry season) and 80% from April to September (the wet season) (Zhao, 1990).

2.2. Field sampling

Two surveys were conducted at 23 stations located in the PRE and in the adjacent area in November 2011 (autumn) and in March 2012 (spring) (Fig. 1). Water samples were collected at a depth of 0.5 m and analyzed for dissolved O_2 (DO), pH, transparency, dissolved nutrients, and phytoplankton pigments. A filtered subsample with a pre-ignited Whatman GF/F filter was added with 0.3% chloroform (final concentration) to determine dissolved nutrients. The filtrate was stored at −20°C in an 80 mL polycarbonate bottle for later analysis. A 1000 mL subsample was filtered on a Whatman GF/F filter with a vacuum pressure of less than 0.03 MPa under low light to analyze phytoplankton pigments. The filters were wrapped in aluminum foil and stored at −80°C for later extraction and analysis of pigments.

2.3. Measurements of environment variables and pigments

Water temperature and salinity were measured using a multiparameter water quality monitoring instrument (YSI 6600, Yellow Springs Instruments, USA). Dissolved oxygen (DO) was analyzed using the Winkler method and the pH with electrode method on board. Water transparency was determined using a Secchi disk. The concentrations of dissolved nutrients, including nitrate, nitrite, ammonium, phosphate, and silicate, were analyzed using a SKALAR flow analyzer in accordance with standard methods (Grasshoff et al., 1983). Dissolved inorganic nitrogen (DIN) was calculated as the sum of nitrate, nitrite, and ammonium.

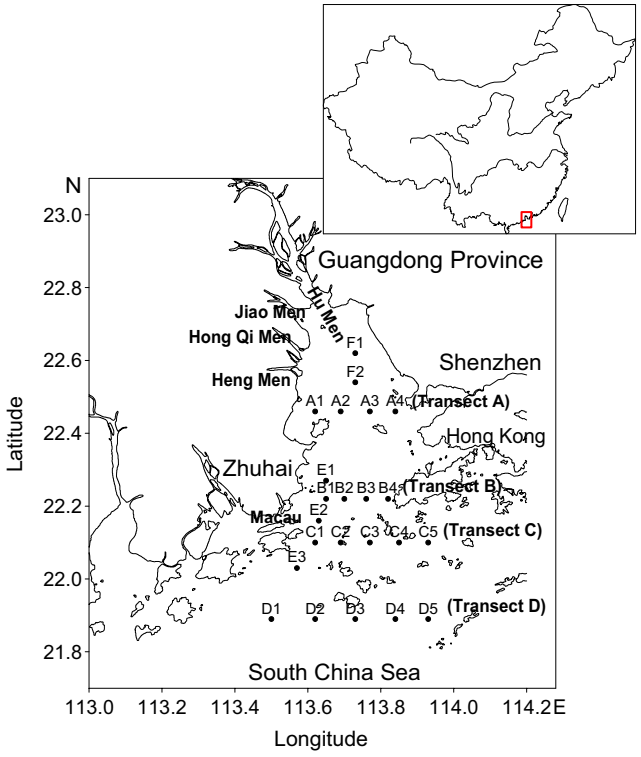

Figure 1 Sampling stations in the PRE in spring and autumn.

Pigment extraction and analysis were conducted according to the methods described by Zapata et al. (2000). The frozen filters were cut into small pieces and then extracted with 3 mL 95% methanol (v/v in deionized water) in a sonication bath with ice and water for 5 min under low light. The extract was then passed through a Teflon film with 0.2 μm pore size to remove cellular debris. The methanol extract (1 mL) was mixed with 0.2 mL Milli-Q water, and then, a 100 μL aliquot of the mixture was analyzed using reverse-phase HPLC.

The HPLC system was equipped with a C8 column (Eclipse XDB, 150 mm × 4.6 mm, 3.5 μm particle size, 1000 nm pore size). The column was maintained at 25°C, and the detection wavelengths of the Agilent diode array detector were set to 430, 440, and 450 nm. Eluent A comprised a methanol:acetonitrile:aqueous pyridine solution (50:25:25, v/v/v), and eluent B was composed of acetonitrile:acetone (80:20, v/v). Elution was performed at a rate of 1.0 mL min^{-1}.

Pigments were identified and quantified using pure pigment standards that contain the following 22 pigments commercially obtained from DHI Inc. (Denmark): chlorophyll *a* (Chl *a*), chlorophyll *b* (Chl *b*), chlorophyll c_2 (Chl c_2), chlorophyll c_3 (Chl c_3), fucoxanthin (Fuco), diadinoxanthin (Diadino), peridinin (Peri), violaxanthin (Viola), alloxanthin (Allo), diatoxanthin (Diato), β,β-carotene (ββ-Car), prasinoxanthin (Pras), lutein (Lut), neoxanthin (Neo), zeaxanthin (Zea), 19′-hex-fucoxanthin (Hex-Fuco), 19′-but-fucoxanthin (But-Fuco), pheophorbide *a* (Pheide *a*), canthaxanthin (Cantha), divinyl chlorophyll *a* (DV-Chl *a*), pheophytin *a* (Phe *a*), and Mg-2,4-divinylpheoporphyrin (MgDVP). Chlorophylls and carotenoids were detected using a diode array detector at 350–750 nm, and chlorophylls were detected by fluorescence at 440 nm and 660 nm (excitation and emission). Absorbance chromatograms were extracted at wavelengths of 430, 440, and 450 nm.

2.4. Pigment indices

Pigment indices included PSC, PPC, and DP. PSC was the sum of Fuco, Peri, Hex-Fuco, But-Fuco, Viola, and Chl *b* (Gibb et al., 2001); and PPC was the sum of Allo, Diadino, Diato, Zea, and ββ-Car (Jeffrey et al., 2005). DP was the sum of seven pigments (Zea, Chl *b*, Allo, Hex-Fuco, But-Fuco, Fuco, and Peri). Among these pigments, Zea and Chl *b* were the signatures of picophytoplankton; Allo, Hex-Fuco, and But-Fuco were those of nanophytoplankton; and Fuco and Peri were those of microphytoplankton. The biomass proportion (BP) of each size group, namely, BP_m (microphytoplankton), BP_n (nanophytoplankton), and BP_p (picophytoplankton), was calculated as follows (Jeffrey et al., 2005):

$$BP_m = \frac{(Fuco + Peri)}{DP} \times 100\%,$$

$$BP_n = \frac{(Allo + Hex\text{-}Fuco + But\text{-}Fuco)}{DP} \times 100\%,$$

$$BP_p = \frac{(Chl\ b + Zea)}{DP} \times 100\%.$$

2.5. Statistical analysis

Principal component analysis (PCA) was applied using SPSS 16.0, and 11 variables (temperature, salinity, pH, DO, transparency, nitrate, nitrite, ammonium, DIN, phosphate, and silicate) were considered to elucidate the main environmental driving force in the PRE. All variables were log-transformed to normalize their distributions. Principal components (PCs) with an eigenvalue of more than 1 were extracted. A rotation of varimax with Kaiser normalization was used to achieve a simpler and more meaningful representation of the underlying PCs. The scores of the PCs and diagnostic pigments were subjected to stepwise multiple linear regression analysis to identify the influencing environmental factors. Correlation was analyzed with the Pearson correlation, and was performed at significance levels of $P < 0.05$ and $P < 0.01$, which indicates that the correlation coefficient outstrips the critical value at the confidence intervals of 95% and 99%, respectively. Standard one-way ANOVA was used to completely randomize the experimental design, and significantly different means were separated ($P = 0.05$).

3. Results

3.1. Hydrological parameters and nutrients

Water temperature was significantly lower but transparency was higher in the spring cruise than in the autumn cruise ($P < 0.05$, Table 1). No significant difference in DO and pH was detected between the two cruises ($P > 0.05$). The mean of phosphate in spring was 0.42 μmol L^{-1}, which was significantly lower than that in autumn ($P < 0.05$). However, DIN (58.47–79.25 μmol L^{-1}) and silicate (39.93–49.38 μmol L^{-1}) did not present significant differences between the two cruises ($P > 0.05$). The high N:P ratio suggested potential phosphorus limitation in the PRE. The distribution of salinity was low in the northwest but high in the southeast, both in spring and autumn (Fig. 2), whereas nitrate and silicate decreased from the northwest to the southeast in the two cruises. Phosphate presented a low concentration in the south in spring and in the middle in autumn.

By applying PCA, 90% and 70% of the variance contained in the original data set was explained by only two PCs in spring and autumn, respectively. Loadings of two PCs are displayed

Table 1 Physio-chemical variables and pigment concentrations from the surface waters of the PRE in spring and autumn.

Physio-chemical variables and pigments	Spring				Autumn			
	AVE	SD	MIN	MAX	AVE	SD	MIN	MAX
Physio-chemical variables								
Temperature [°C]	17.19	0.3	16.49	17.82	23.95	0.36	23.15	24.66
Salinity	26.86	6.15	12.57	32.58	25.77	6.38	10.17	33.36
DO [mg L^{-1}]	7.94	0.41	6.96	8.66	6.69	0.31	5.89	7.41
pH	8.13	0.17	7.76	8.33	7.81	0.14	7.46	8.03
Transparency [m]	1.2	0.9	0.2	3.2	0.8	0.3	0.5	2.0
Nitrate [μmol L^{-1}]	35.17	28.38	3.76	93	60.28	49.97	4.81	177.18
Nitrite [μmol L^{-1}]	6.62	5.76	0.56	19.91	13.06	7.52	2.49	32.02
Ammonium [μmol L^{-1}]	16.67	12.61	0.27	32.7	5.9	3.26	2.26	14.71
DIN [μmol L^{-1}]	58.47	44.21	4.65	140.75	79.25	55.63	12.62	201.27
Phosphate [μmol L^{-1}]	0.42	0.3	0.08	0.98	0.82	0.41	0.35	2.46
Silicate [μmol L^{-1}]	49.38	38.32	7.96	137.96	39.93	23.93	7.78	78.27
DIN:phosphate ratio	137.60	81.53	43.30	443.59	103.66	69.89	11.40	240.06
Pigments								
Chl *a* [μg L^{-1}]	1.166	1.605	0.126	7.712	0.267	0.141	0.013	0.570
Chl *b* [μg L^{-1}]	0.029	0.041	0.000	0.140	0.070	0.030	0.023	0.127
Chl c_2 [μg L^{-1}]	0.859	0.710	0.143	3.437	0.040	0.029	0.000	0.096
Chl c_3 [μg L^{-1}]	0.054	0.058	0.000	0.190	0.006	0.010	0.000	0.045
Fuco [μg L^{-1}]	2.914	3.103	0.148	11.020	0.207	0.073	0.075	0.332
Diadino [μg L^{-1}]	0.261	0.240	0.057	1.082	0.028	0.013	0.010	0.059
Peri [μg L^{-1}]	0.208	0.157	0.027	0.565	0.061	0.029	0.017	0.123
Viola [μg L^{-1}]	0.019	0.010	0.006	0.043	0.011	0.004	0.005	0.018
Allo [μg L^{-1}]	0.131	0.082	0.050	0.328	0.052	0.028	0.003	0.107
Diato [μg L^{-1}]	0.042	0.026	0.012	0.113	0.005	0.004	0.000	0.012
ββ-Car [μg L^{-1}]	0.037	0.049	0.000	0.212	0.007	0.005	0.000	0.013
Pras [μg L^{-1}]	0.023	0.015	0.000	0.056	0.011	0.007	0.002	0.029
Lut [μg L^{-1}]	0.019	0.014	0.005	0.061	0.008	0.005	0.000	0.019
Neo [μg L^{-1}]	0.016	0.011	0.000	0.037	0.012	0.005	0.002	0.026
Zea [μg L^{-1}]	0.013	0.009	0.002	0.031	0.017	0.011	0.007	0.043
Hex-Fuco [μg L^{-1}]	0.019	0.018	0.000	0.058	0.012	0.010	0.000	0.036
But-Fuco [μg L^{-1}]	0.002	0.002	0.000	0.008	0.004	0.003	0.000	0.011

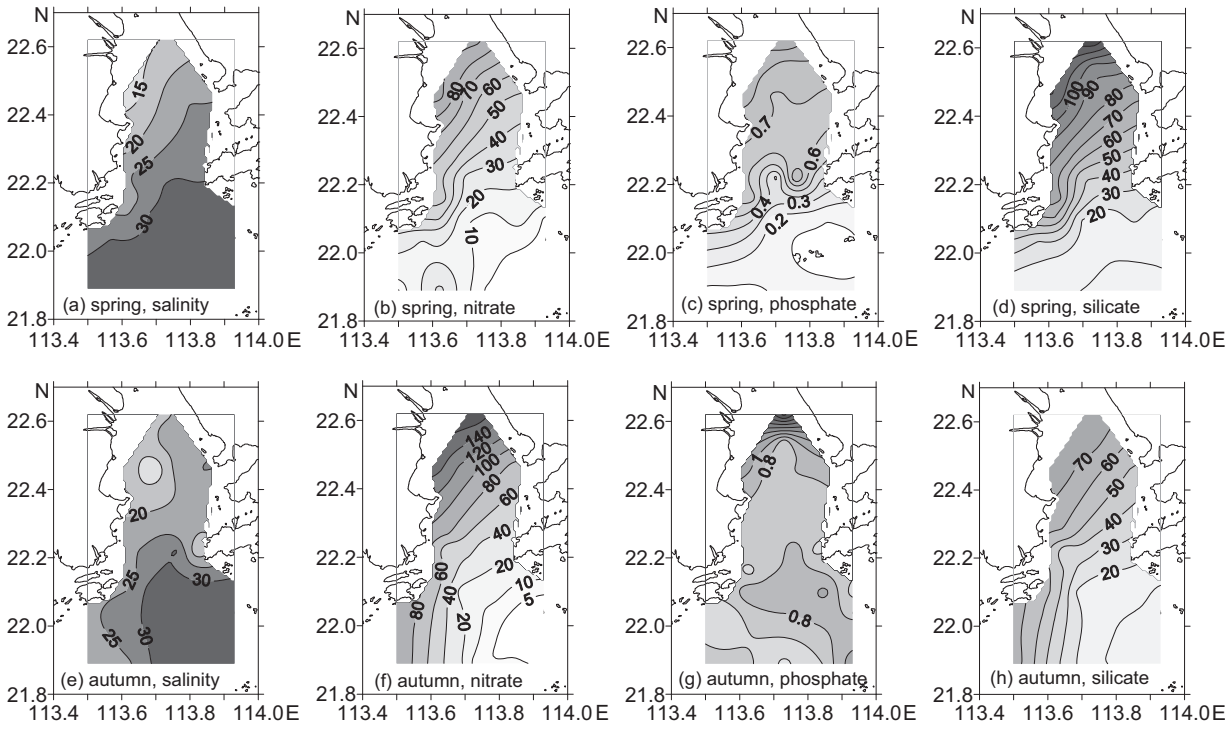

Figure 2 Spatial distributions of salinity and nutrients [μmol L^{-1}] in the PRE in spring and autumn.

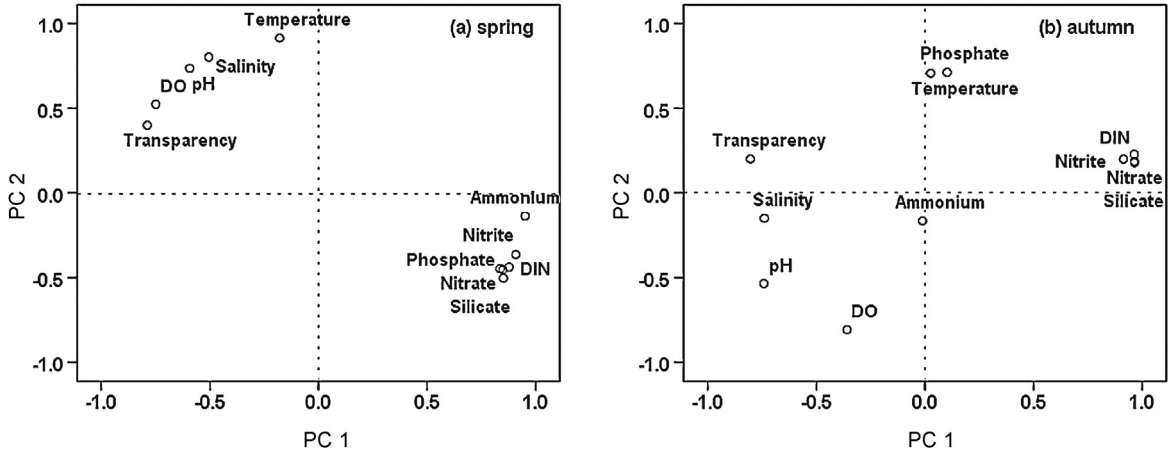

Figure 3 Loadings of 11 variables on two rotated PCs in (a) spring and (b) autumn.

in Fig. 3. In spring, PC 1 was highly participated by nutrients, whereas PC 2 was mainly participated by water temperature, salinity, and pH. Similarly, PC 1 had a highly positive load of nitrogen and silicon in autumn, whereas PC 2 had load of water temperature and phosphate. The results from Pearson's correlation (Table 2) showed that all nutrients correlated most significantly with PC 1 in spring ($r > 0.8$, $P < 0.01$), whereas nitrogen and silicon correlated significantly with PC 1 in autumn ($r > 0.9$, $P < 0.01$). Thus, nutrients were the most important environmental driving element in the PRE. In addition, the high correlation coefficients between PC 2 and temperature and salinity in spring, as well as between PC 1 and transparency in autumn, indicated that these physical variables were also important.

3.2. Pigment concentrations and distributions

Among 22 pigments, 17 major pigments were detected in the PRE during the sampling periods (Table 1). Chl *a*, Fuco, and Chl c_2 were the most abundant pigments in spring, with mean values of 1.166, 2.914, and 0.859 μg L^{-1}, respectively. By comparison, the concentrations of Diadino, Peri, and Allo were relatively low, i.e., 0.131–0.261 μg L^{-1}; the other 11 pigments were <0.1 μg L^{-1} in concentration. In autumn, the mean values of Chl *a* and Fuco were higher than those of the other pigments, which were 0.267 μg L^{-1} and 0.207 μg L^{-1}, respectively. By contrast, the mean values of Chl *b*, Peri, and Allo were lower, i.e., 0.052–0.070 μg L^{-1}. Other pigments had relatively low concentrations, with mean values generally

Table 2 Pearson's correlation coefficients between the variables and PCs.

	Spring		Autumn	
	PC 1	PC 2	PC 1	PC 2
Temperature	−0.179	0.913**	0.026	0.705**
Salinity	−0.505*	0.800**	−0.740**	−0.151
DO	−0.749**	0.523*	−0.359	−0.735**
pH	−0.593**	0.735**	−0.742**	−0.535**
Transparency	−0.788**	0.399	−0.804**	0.200
Nitrate	0.849**	−0.453*	0.964**	0.187
Nitrite	0.878**	−0.438*	0.914**	0.199
Ammonium	0.951**	−0.137	−0.011	−0.166
DIN	0.909**	−0.364	0.963**	0.227
Phosphate	0.837**	−0.448*	0.102	0.711**
Silicate	0.852**	−0.503*	0.965**	0.178

* $P < 0.05$.
** $P < 0.01$.

lower than 0.02 μg L^{-1}. Significant differences in the concentrations of pigments, except in Neo, Zea, and Hex-Fuco, were determined between the two cruises. The concentrations of nearly all pigments, except Chl *b* and But-Fuco, were significantly higher in spring than in autumn ($P < 0.05$). MgDVP, Pheide *a*, Cantha, DV-Chl *a*, and Phe *a* were not detected in the PRE during the two cruises.

The spatial distribution of Chl *a* and diagnostic pigments in spring and in autumn is presented in Figs. 4 and 5, respectively, while other pigments are not showed. Chl *a*, Chl c_2, Fuco, Diadino, Diato, and ββ-Car exhibited a similar distribution, i.e., higher in the northern or northwest estuary but lower in the south. Except Fuco, which is the characteristic pigment of diatoms, Chl *a*, Chl c_2, Diadino, Diato, and ββ-Car were observed in many phytoplankton species. Their distributions were obviously influenced by diluted water. The highest values of Chl *a*, Fuco, Diadino, and ββ-Car were observed at station A2, and those of Chl c_2 and Diato at stations F1 and F2. By contrast, Peri, the characteristic pigment of dinoflagellates, was mainly distributed in the northeast and south estuary. Chl *b*, Chl c_3, Allo, Pras, Lut, Neo, Hex-Fuco, and But-Fuco were distributed at high concentrations in the southern part of the sampling region; these pigments were mainly found at station D3 or D5. The concentrations of Viola and Zea were high in the north and south, but low in the central part of the estuary.

Unlike in spring, Chl *a*, Chl c_2, Fuco, Diadino, Diato, Allo, and But-Fuco showed high concentrations in the middle eastern and northeast parts of the sampling region, with the highest value in station B4. Similar to the pigments in spring, Chl *b*, Chl c_3, Pras, and Zea in autumn were distributed in the southern part, with the highest value in station D4 or D2. Furthermore, Peri in autumn presented the same distribution as that in spring, whose high value was distributed both in the northeast and in the south.

Correlation analysis showed that Chl *a* in spring was significantly positively correlated with Fuco ($r = 0.587$, $P < 0.01$). In addition, Chl *a* and Fuco were significantly negatively correlated with salinity ($r = -0.504$ and -0.768, respectively, $P < 0.05$) but significantly positively correlated with nutrients ($r = 0.444$–0.752, $P < 0.05$). By contrast, Hex-Fuco and But-Fuco were significantly positively correlated with salinity ($r = 0.555$ and 0.436, respectively, $P < 0.05$) but significantly negatively correlated with nutrients ($r = -0.491$ to -0.682, $P < 0.05$). Unlike in spring, Chl *a* in autumn was significantly positively correlated with Allo, Chl *b*, and Zea ($r = 0.436$–0.753, $P < 0.05$). Allo, Chl *b*, and Zea were significantly positively correlated with salinity ($r = 0.419$–0.598,

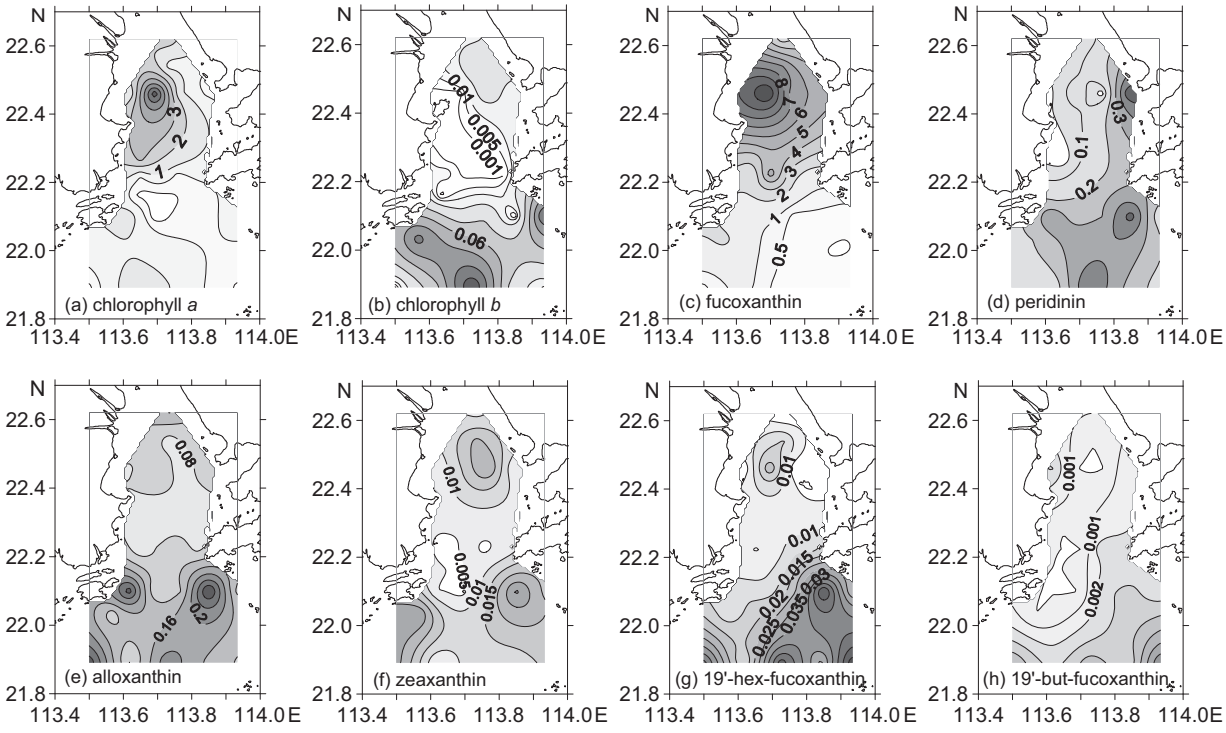

Figure 4 Spatial distributions of pigments in the PRE in spring [μg L^{-1}].

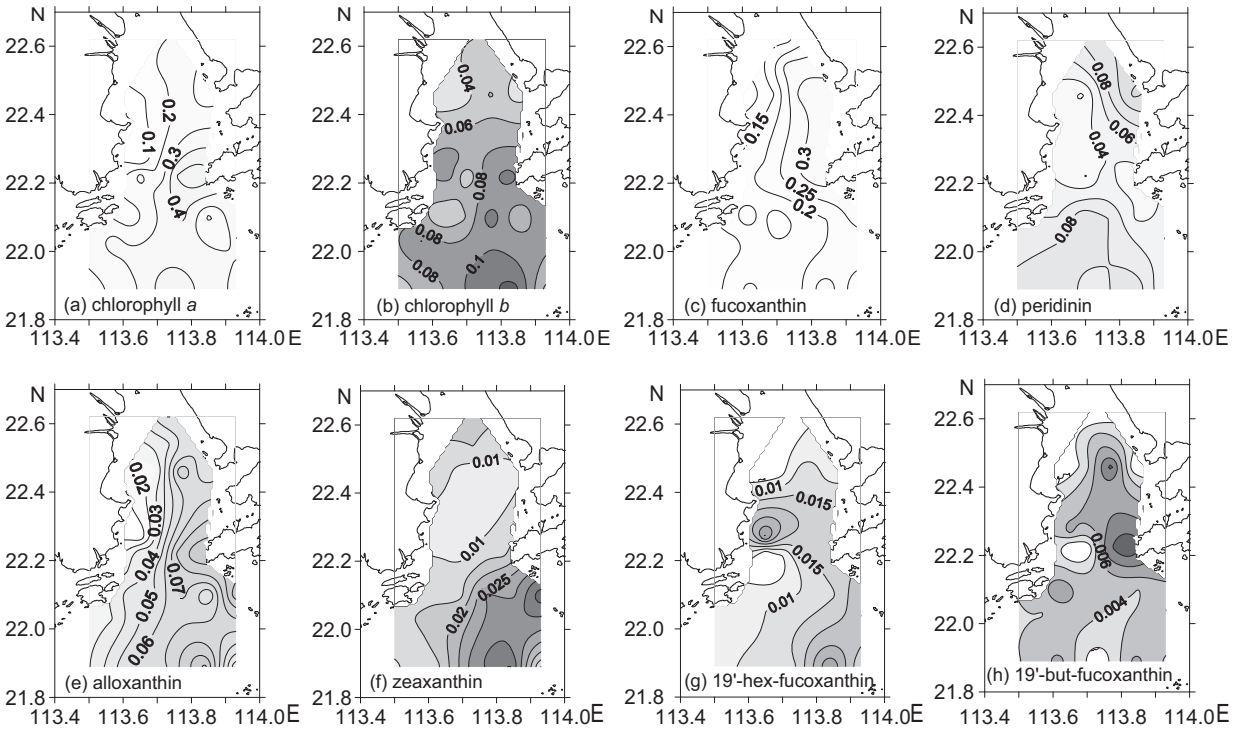

Figure 5 Spatial distributions of pigments in the PRE in autumn [$\mu g\ L^{-1}$].

$P < 0.05$), whereas Chl *a*, Allo, Hex-Fuco, Chl *b*, and Zea were significantly negatively correlated with nitrate and silicate ($r = -0.468$ to -0.625, $P < 0.05$).

3.3. Phytoplankton pigment indices

The mean of BP_m in spring was 85.4%, and ranged from 55.3% to 99.1%, which was higher than that in autumn with a mean of 64.1%. By contrast, the mean of BP_p in autumn (20.6%) was significantly higher than that in spring (3.3%). In spring, BP_m was higher in the area with salinity <30, but BP_p and BP_n were higher in the area with salinity >30 (Fig. 6). BP_m generally increased but BP_p and BP_n reduced with the increase in nitrate, phosphate, and silicate. Similar to spring, BP_m increased but BP_n decreased with increasing nitrate and silicate. However, no relationship was found between BP_p and salinity or nutrients as well as between phosphate and any BP in autumn.

The PPC:PSC ratios in most stations of transects C and D in spring approached the unity linear relationship (red line, in Fig. 7), but were low in stations A1 to A4, B2, and F2. By comparison, the PPC:PSC ratios in all stations were under the unity line in autumn.

4. Discussion

4.1. Phytoplankton diversity and distribution in the PRE as revealed by pigments

High concentrations of Fuco and Peri during two cruises confirmed that diatoms and dinoflagellates were dominant, and the detected pigments, including Allo, Pras, Lut, Zea, Hex-Fuco, and But-Fuco, indicated the presence of cryptophytes, prasinophytes, chlorophytes, cyanophytes, haptophytes, and pelagophytes. By contrast, DV-Chl *a* with an undetectable level implied that no *Prochlorococcus* was present during sampling time.

The distribution of pigments implies the spatial variations of phytoplankton. In spring, the high value of Chl *a* and Fuco suggested the existence of a diatom bloom in the north of the estuary. The distributions of Chl *b*, Allo, Pras, Lut, Hex-Fuco, and But-Fuco indicated that cryptophytes, chlorophytes, prasinophytes, haptophytes, and pelagophytes mainly existed in the south. The distributions of Peri and Zea indicated that dinoflagellates and cyanophytes basically existed both in the north and south but were low in the central part. Similar to spring, dinoflagellates in autumn were mainly distributed both in the northeast and in the south, while chlorophytes and cyanophytes were mainly distributed in the south. However, unlike in spring, diatoms, cryptophytes, and pelagophytes mainly existed in the middle-eastern and northeast parts of the estuary. The phytoplankton distribution found in the current study is consistent with those in previous studies (Harrison et al., 2008; Lu and Gan, 2015; Yin, 2003). Temperature, light, hydrodynamics, and nutrient supply are the major factors that control the spatial–temporal distribution of phytoplankton (Agawin et al., 2000; Marañón et al., 2007; Riegman et al., 1993). Lu and Gan (2015) found that the low river discharge leads to longer water residence time, satisfactory water column stability, and transparency, which are helpful for the diatom bloom in the upper PRE during the dry season. In the present study, higher salinity in spring indicated low river discharge, which may result in diatom bloom in the northern estuary during spring (Table 1). As for the spatial distribution, Li et al. (2013) and Zhang et al. (2013) reported that larger phytoplankton (e.g., diatom) are

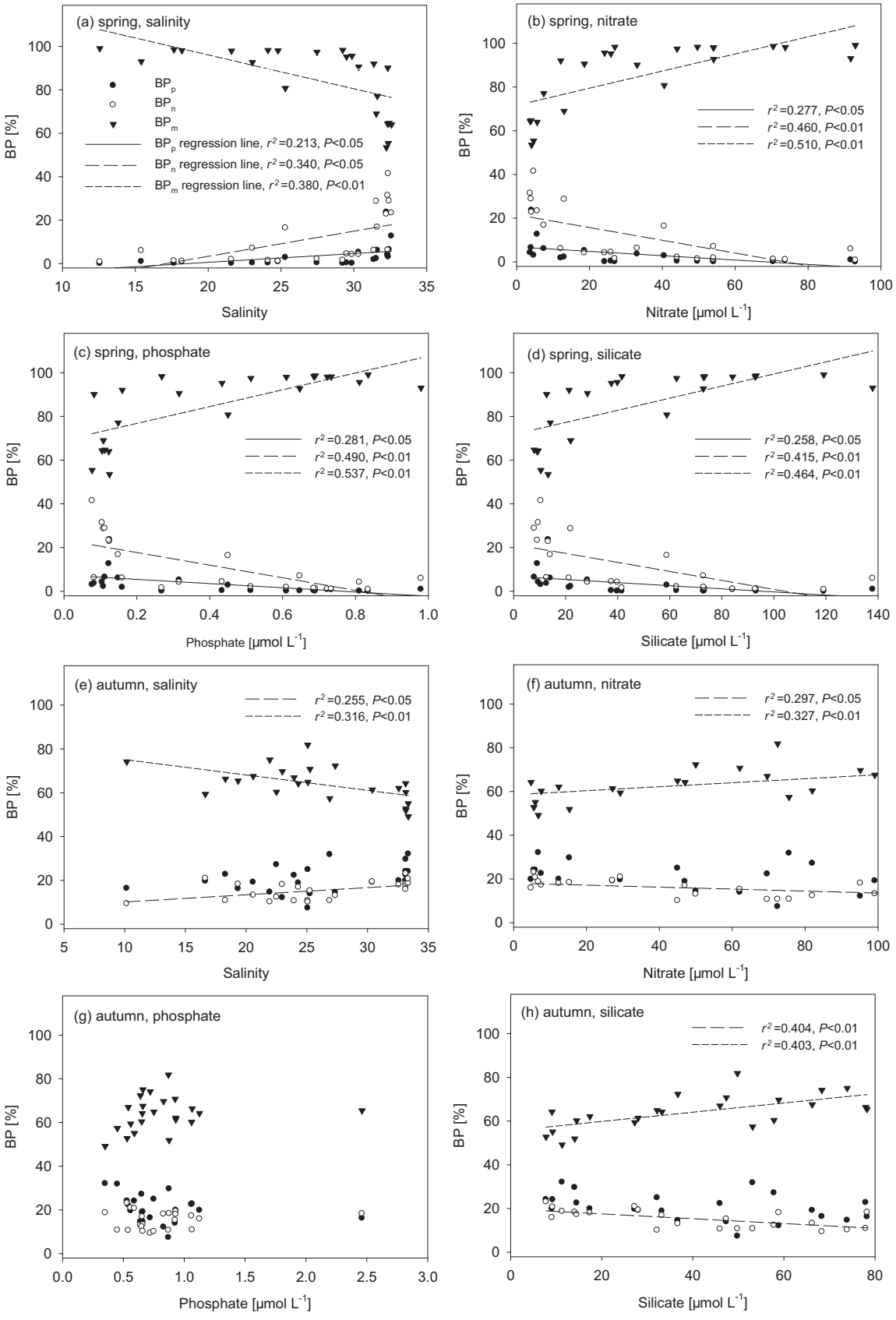

Figure 6 Relationship of BP with environmental variables in the PRE in spring and autumn.

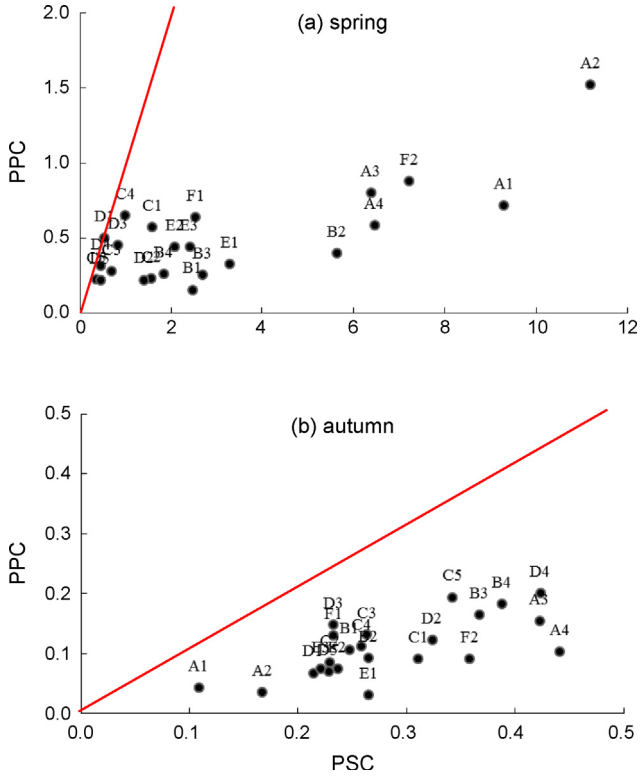

Figure 7 PPC vs. PSC by station numbers in the PRE in (a) spring and (b) autumn. The red line denotes the unity line, which indicates that PPC:PSC is 1. (For interpretation of the references to color in this figure legend, the reader is referred to the web version of this article.)

Table 3 Regression analysis of the principal component scores (as independent factors) for the diagnostic pigments in spring and autumn[a].

Dependent factor	R^2	F	β	
			PC 1	PC 2
Spring				
Fuco	0.563**	12.880	0.609**	−0.438**
Peri	0.199	2.491	−0.085	0.438*
Allo	0.134	1.548	−0.306	0.201
Zea	0.104	1.336	−0.195	0.258
Chl *b*	0.203	2.544	−0.269	0.361
Hex-Fuco	0.607**	15.435	−0.751**	0.205
But-Fuco	0.551**	12.251	−0.741**	0.309
Autumn				
Fuco	0.027	0.274	−0.159	−0.036
Peri	0.154	1.825	−0.081	−0.384
Allo	0.397**	6.595	−0.615**	0.140
Zea	0.521**	10.888	−0.722**	−0.111
Chl *b*	0.484**	9.366	−0.541**	−0.437*
Hex-Fuco	0.301*	4.414	−0.516*	−0.188
But-Fuco	0.060	0.639	−0.181	−0.165

[a] R^2: regression coefficient; β: F-value of the full model and the standardized coefficient.
* $P < 0.05$.
** $P < 0.01$.

dominant in the upper PRE that has low salinity and high nutrient content, whereas the smaller ones (e.g., blue-green algae) are found in water with high salinity and low nutrient content. Stepwise multiple regression analysis indicated that Fuco positively correlated, whereas Hex-Fuco, Allo, Zea, and Chl *b* negatively correlated with PC 1, indicating that nutrients were the main environmental controlling factors (Table 3).

4.2. Relationship of different phytoplankton groups as revealed by pigments with environmental factors

The biomass proportions derived from pigments suggest the size structure of phytoplankton. In this study, BP_m was considerably higher than BP_n and BP_p in the area with salinity <30, and BP_n increased, particularly in spring, despite the decrease in BP_m in the area with salinity >30 (Fig. 6). Therefore, high BP_m and BP_n indicated the dominance of microphytoplankton and nanophytoplankton in the PRE. This result is consistent with previous investigations conducted through microscopy and flow cytometry (Qiu et al., 2010). In comparison, the increasing BP_p in the area with salinity >30 in spring indicated that picophytoplankton became abundant (Fig. 6), and the increase in BP_p in autumn suggested the abundance of picophytoplankton. Phytoplankton sizes are generally affected by environmental factors (Finkel et al., 2007, 2009). Large phytoplanktons are generally developed in turbulent and high nutrient waters (Huete-Ortega et al., 2010; Margalef, 1978; Reul et al., 2006), whereas small phytoplanktons are developed in stratified and low nutrient waters (Chisholm, 1992; Kiørboe, 1993; Marañon, 2009). With the decrease in nutrient availability, phytoplankton typically change from a large species to small one (Roy et al., 2006); thus, microphytoplankton generally dominate areas in nutrient-rich conditions (Chen and Liu, 2010). By comparison, nanophytoplankton and picophytoplankton are abundant in nutrient-deficient waters (Roy et al., 2006; Thingstad, 1998), although they contribute to the total biomass in nutrient-rich coastal waters (Badylak and Phlips, 2004; Phlips et al., 1999). In the present study, BP_n and BP_p increased but BP_m decreased with decreasing nutrient concentration in spring (Fig. 6). This result indicates that nutrient concentration influences phytoplankton distribution with different sizes. A previous study also reported that the abundance of picophytoplankton in the PRE is negatively correlated with inorganic nutrients (Zhang et al., 2013). This report implies that low nutrient concentrations in offshore areas promote the growth of picophytoplankton.

4.3. Influence of environmental factors on PPC and PSC

Environmental and trophic conditions affect PPC and PSC, which function as indicators of the physiological condition of a phytoplankton community (Trees et al., 2000; Veldhuis and Kraay, 2004). Lutz et al. (2003) noted an increase in PPC at

high irradiance levels while the elevated proportion of PSC at low irradiance, and Barlow et al. (2007) found that PPC is dominated where nitrate concentrations are $<0.007\ \mu mol\ L^{-1}$, but PSC is high at nitrate levels $>0.007\ \mu mol\ L^{-1}$. As a result, intensive light and low nutrients increase the proportion of PPC, and consequently, the ratio of PPC:PSC (Moreno et al., 2012; Vijayan et al., 2009). In the present study, the nutrient concentration in the southern part was low in spring (Fig. 2); meanwhile, the average transparency was 1.98 m in transects C and D, which was considerably higher than that in transect A (0.2 m), inferring adequate light in transects C and D during spring. Therefore, adequate light and low nutrients may increase PPC:PSC ratios in the southern part (transects C and D) of the PRE in spring (Fig. 7).

By comparison, environmental variables between autumn and spring showed nonsignificant differences ($P > 0.05$), except water temperature, which was significantly lower in spring than in autumn. Higher phytoplankton biomass and more samples of higher PPC:PSC ratio were observed during spring despite lower water temperature (Table 1, Fig. 7). These trends were probably due to the satisfactory water transparency in spring. Average transparency was 1.2 m during spring but was only 0.8 m during autumn (Table 1). Higher transparency may result in adequate light intensity, possibly causing high levels of the pigments and PPC:PSC ratios during spring. Zhang et al. (2014) also reported that turbidity and light are principal factors that affect phytoplankton biomass in the PRE. Therefore, the spatial–temporal distribution of PPC:PSC ratios provides information on the physiological condition of the phytoplankton community in the PRE as influenced by light, transparency, and nutrient conditions. On this basis, PPC:PSC ratio can be used as a classification tool for ecosystems because it can be related both to phytoplankton populations and to hydrography (Moreno et al., 2012).

5. Conclusion

Among the 22 pigments, 17 were detected using HPLC. Fuco was the most abundant accessory pigment. The detected pigments indicated the presence of diatoms, dinoflagellates, cryptophytes, prasinophytes, chlorophytes, cyanophytes, haptophytes, and pelagophytes. Most pigment levels were significantly higher in spring than in autumn, and different spatial distribution patterns were presented between the two seasons.

The salinity and nutrient levels influenced the distribution of phytoplankton functional types in the PRE. BP_m was higher during spring, whereas BP_p was higher during autumn. BP_m in spring was high in areas with salinity <30, whereas BP_p and BP_n were high in areas with salinity >30. BP_m increased whereas BP_n reduced with the increase in nutrient contents. By comparison, BP_p declined with the increase in nutrient contents during spring.

The PPC:PSC ratios in the southern estuary approached unity linear relationship during spring and were under the unity line during autumn. PPC:PSC ratios provide an estimate of the physiological condition of the phytoplankton community in the PRE as influenced by light, transparency, and nutrients conditions.

References

Agawin, N.R.S., Duarte, C.M., Agustí, S., 2000. Nutrient and temperature control of the contribution of picoplankton to phytoplankton biomass and production. Limnol. Oceanogr. 45 (3), 591–600.

Aneeshkumar, N., Sujatha, C.H., 2012. Biomarker pigment signatures in Cochin back water system – a tropical estuary south west coast of India. Estuar. Coast. Shelf Sci. 99, 182–190.

Badylak, S., Phlips, E.J., 2004. Spatial and temporal patterns of phytoplankton composition in a subtropical coastal lagoon, the Indian River Lagoon, Florida, USA. J. Plankton Res. 26 (10), 1229–1247.

Barlow, R.G., Aiken, J., Holligan, P.M., Cummings, D.G., Maritorena, S., Hooker, S., 2002. Phytoplankton pigment and absorption characteristics along meridional transects in the Atlantic Ocean. Deep-Sea Res. Pt. I 49 (4), 637–660.

Barlow, R., Kyewalyanga, M., Sessions, H., Van den Berg, M., Morris, T., 2008. Phytoplankton pigments, functional types, and absorption properties in the Delagoa and Natal Bights of the Agulhas ecosystem. Estuar. Coast. Shelf Sci. 80 (2), 201–211.

Barlow, R., Stuart, V., Lutz, V., Sessions, H., Sathyendranath, S., Platt, T., Kyewalyanga, M., Clementson, L., Fukasawa, M., Watanabe, S., Devred, E., 2007. Seasonal pigment patterns of surface phytoplankton in the subtropical southern hemisphere. Deep-Sea Res. Pt. I 54 (10), 1687–1703.

Bulletin of Water Resources in the Pearl River Drainage, 2011. Commission of Water Resources of Pearl River, Ministry of Water Resources of the People's Republic of China, http://www.pearlwater.gov.cn/xxcx/szygg/.

Bulletin of Water Resources in the Pearl River Drainage, 2012. Commission of Water Resources of Pearl River, Ministry of Water Resources of the People's Republic of China, http://www.pearlwater.gov.cn/xxcx/szygg/.

Chen, B.Z., Liu, H.B., 2010. Relationships between phytoplankton growth and cell size in surface oceans: interactive effects of temperature, nutrients, and grazing. Limnol. Oceanogr. 55 (3), 965–972.

Chisholm, S.W., 1992. Phytoplankton size. In: Falkowski, P.G., Woodheard, A.D. (Eds.), Primary Productivity and Biogeochemical Cycles in the Sea. Plenum Press, New York, 213–238.

Finkel, Z.V., Sebbo, J., Feist-Burkhardt, S., Irwin, A.J., Katz, M.E., Schofield, O.M.E., Falkowksi, P.G., 2007. A universal driver of macroevolutionary change in the size of marine phytoplankton over the Cenozoic. Proc. Natl. Acad. Sci. U.S.A. 104, 20416–20420.

Finkel, Z.V., Vaillancourt, C.J., Irwin, A.J., Reavie, E.D., Smol, J.P., 2009. Environmental control of diatom community size structure varies across aquatic ecosystems. Proc. R. Soc. B 276, 1627–1634.

Gibb, S.W., Barlow, R.G., Cummings, D.G., Rees, N.W., Trees, C.C., Holligan, P., Suggett, D., 2000. Surface phytoplankton pigment distributions in the Atlantic Ocean: an assessment of basin scale variability between 50°N and 50°S. Prog. Oceanogr. 45 (3–4), 339–368.

Gibb, S.W., Cummings, D.G., Irigoien, X., Barlow, R.G., Fauzi, R., Mantoura, C., 2001. Phytoplankton pigment chemotaxonomy of northeastern Atlantic. Deep-Sea Res. Pt. II 48 (4–5), 795–823.

Grasshoff, K., Erhardt, M., Kremiling, K., 1983. Methods of Seawater Analysis. Verlag Chemie, Wienhien, 632 pp.

Harrison, P.J., Yin, K.D., Lee, J.H.W., Gan, J.P., Liu, H.B., 2008. Physical–biological coupling in the Pearl River Estuary. Cont. Shelf Res. 28 (12), 1405–1415.

He, B.Y., Dai, M.H., Zhai, W.D., Guo, X.H., Wang, L.F., 2014. Hypoxia in the upper reaches of the Pearl River Estuary and its maintenance mechanisms: a synthesis based on multiple year observations during 2000–2008. Mar. Chem. 167 (20), 13–24.

Huang, L.M., Jian, W.J., Song, X.Y., Huang, X.P., Liu, S., Qian, P.Y., Yin, K.D., Wu, M., 2004. Species diversity and distribution for phytoplankton of the Pearl River estuary during rainy and dry seasons. Mar. Pollut. Bull. 49 (7–8), 588–596.

Huete-Ortega, M., Marañon, E., Varela, M., Bode, A., 2010. General patterns in the size scaling of phytoplankton abundance in coastal waters during a 10-year time series. J. Plankton Res. 32 (1), 1—14.

Jeffrey, S.W., Mantoura, R.F.C., Bjørnland, T., 1997. Data for the identification of 47 key phytoplankton pigments. In: Jeffrey, S.W., Mantoura, R.F.C., Wright, S.W. (Eds.), Phytoplankton Pigments in Oceanography: Guidelines to Modern Methods. Monographs on Oceanographic Methodology. UNESCO, Paris, 449—559.

Jeffrey, S., Mantoura, R., Wright, S. (Eds.), 2005. Phytoplankton Pigments in Oceanography. Guidelines to Modern Methods. Monographs on Oceanographic Methodology, 2nd edn. UNESCO, Paris, 661 pp.

Kiørboe, T., 1993. Turbulence, phytoplankton cell size, and the structure of pelagic food webs. Adv. Mar. Biol. 29, 1—72.

Lerman, A., 1981. Control on river water composition and the mass balance of river systems. In: Martin, J.M., Burton, J.D., Eisma, D. (Eds.), River Inputs to Ocean Systems. Proceedings of a SCOR/ACMRR/ECOR/IAHS/UNESCO/CMG/IABO/IAPSO Review and Workshop, 26—30 March 1979, UNEP and UNESCO, Rome.

Li, G., Lin, Q., Lin, J.D., Song, X.Y., Tan, Y.H., Huang, L.M., 2014. Environmental gradients regulate the spatial variations of phytoplankton biomass and community structure in surface water of the Pearl River estuary. Acta Ecol. Sin. 34 (2), 129—133.

Li, L., Lu, S.H., Jiang, T., Li, X., 2013. Seasonal variation of size-fractionated phytoplankton in the Pearl River estuary. Chin. Sci. Bull. 58 (19), 2303—2314.

Lu, Z.M., Gan, J.P., 2015. Controls of seasonal variability of phytoplankton blooms in the Pearl River Estuary. Deep-Sea Res. Pt. II 117, 86—96.

Lutz, V.A., Sathyendranath, S., Head, E.J.H., Li, W.K.W., 2003. Variability in pigment composition and optical characteristics of phytoplankton in the Labrador Sea and the Central North Atlantic. Mar. Ecol. Prog. Ser. 260, 1—18.

Marañon, E., 2009. Phytoplankton size structure. In: Steele, J.H., Turekian, K.K., Thorpe, S.A. (Eds.), Encyclopedia of Ocean Sciences. 2nd ed. Amsterdam, Elsevier, 445—452.

Marañón, E., Cermeño, P., Rodríguez, J., Zubkov, M.V., Harris, R.P., 2007. Scaling of phytoplankton photosynthesis and cell size in the ocean. Limnol. Oceanogr. 52 (5), 2190—2198.

Margalef, R., 1978. Life forms of phytoplankton as survival alternatives in an unstable environment. Oceanol. Acta 1 (4), 493—509.

Moreno, D.V., Marrero, P., Morales, J., Llerandi García, C., Villagarcía Úbed, M.G., Rueda, M.J., Llinás, O., 2012. Phytoplankton functional community structure in Argentinian continental shelf determined by HPLC pigment signatures. Estuar. Coast. Shelf Sci. 100, 72—81.

Naik, R.K., Anil, A.C., Narale, D.D., Chitari, R.R., Kulkarni, V.V., 2011. Primary description of surface water phytoplankton pigment patterns in the Bay of Bengal. J. Sea Res. 65 (4), 435—441.

Paerl, H.W., Valdes, L.M., Pinckney, J.L., Piehler, M.F., Dyble, J., Moisander, P.H., 2003. Phytoplankton photopigments as indicators of estuarine and coastal eutrophication. BioScience 53 (10), 953—964.

Phlips, E.J., Badylak, S., Lynch, T.C., 1999. Blooms of the picoplanktonic cyanobacterium Synechococcus in Florida Bay, a subtropical inner-shelf lagoon. Limnol. Oceanogr. 44 (4), 1166—1175.

Qiu, D.J., Huang, L.M., Zhang, J.L., Lin, S.J., 2010. Phytoplankton dynamics in and near the highly eutrophic Pearl River Estuary, South China Sea. Cont. Shelf Res. 30 (2), 177—186.

Reul, A., Rodríguez, J., Blanco, J.M., Rees, A.P., Burkill, P.H., 2006. Control of microplankton size structure in contrasting water columns of Celtic Sea. J. Plankton Res. 28 (5), 449—457.

Riegman, R., Kuipers, B.R., Noordeloos, A.A.M., Witte, H.J., 1993. Size-differential control of phytoplankton and the structure of plankton communities. Netherlands J. Sea Res. 31, 255—265.

Roy, R., Pratihary, A., Mangesh, G., Naqvi, S.W.A., 2006. Spatial variation of phytoplankton pigments along the southwest coast of India. Estuar. Coast. Shelf Sci. 69 (1—2), 189—195.

Sieburth, J.M., Smetacek, V., Lenz, J., 1978. Pelagic ecosystem structure: heterotrophic compartments of the plankton and their relationship to plankton size fractions. Limnol. Oceanogr. 23 (6), 1256—1263.

Thingstad, T.F., 1998. Theoretical approach to structuring mechanisms in the pelagic food web. Hydrobiologia 363 (1—3), 59—72.

Trees, C.C., Clark, D.K., Bidigare, R.R., Ondrusek, M.E., Mueller, J. L., 2000. Accessory pigments versus chlorophyll *a* concentrations within the euphotic zone: a ubiquitous relationship. Limnol. Oceanogr. 45 (5), 1130—1143.

Veldhuis, M.J.W., Kraay, G.W., 2004. Phytoplankton in the subtropical Atlantic Ocean: towards a better assessment of biomass and composition. Deep-Sea Res. Pt. I 51 (4), 507—530.

Vidussi, F., Claustre, H., Manca, B., Luchetta, A., Marty, J., 2001. Phytoplankton pigment distribution in relation to upper thermocline circulation in the eastern Mediterranean Sea during winter. J. Geophys. Res. 106 (C9), 19939—19956.

Vijayan, A.K., Yoshikawa, T., Watanabe, S., Sasaki, H., Matsumoto, K., Saito, S.i., Takeda, S., Furuya, K., 2009. Influence on non-photosynthetic pigments on light absorption and quantum yield of photosynthesis in the western equatorial pacific and the subarctic north pacific. J. Oceanogr. 65 (2), 245—258.

Wright, S.W., Jeffrey, S.W., 2006. Pigment markers for phytoplankton production. The Handbook of Environmental Chemistry, vol. 2, Part N. 71—104.

Yin, K., 2003. Influence of monsoons and oceanographic processes on red tides in Hong Kong in the vicinity of the Pearl River Estuary. Mar. Ecol. Prog. Ser. 262, 27—41.

Yin, K., Qian, P.Y., Chen, J.C., Hsieh, D.P., Harrison, P.J., 2000. Dynamics of nutrients and phytoplankton biomass in the Pearl River estuary and adjacent waters of Hong Kong during summer: preliminary evidence for phosphorus and silicon limitation. Mar. Ecol. Prog. Ser. 194, 295—305.

Yin, K., Qian, P.Y., Chen, J.F., Huang, L., Zhang, J., Wu, M., 2004. Effect of wind events on phytoplankton blooms in the Pearl River Estuary during summer. Cont. Shelf Res. 24 (16), 1909—1923.

Yin, K., Qian, P.Y., Wu, M.C.S., Chen, J.C., Huang, L.M., Song, X.Y., Jian, W.J., 2001. Shift from P to N limitation of phytoplankton growth across the Pearl River estuarine plume during summer. Mar. Ecol. Prog. Ser. 221, 17—28.

Zapata, M., Rodríguez, F., Garrido, J.L., 2000. Separation of chlorophylls and carotenoids from marine phytoplankton: a new HPLC method using a reversed phase C8 column and pyridine-containing mobile phases. Mar. Ecol. Prog. Ser. 195, 29—45.

Zhai, W., Dai, M., Cai, W.J., Wang, Y., Wang, Z., 2005. High partial pressure of CO_2 and its maintaining mechanism in a subtropical estuary: the Pearl River estuary, China. Mar. Chem. 93, 21—32.

Zhang, X., Huang, X.P., Shi, Z., Ye, F., Liu, Q.X., 2013. Spatial and temporal variation of picophytoplankton in the Pearl River Estuary. Acta Ecol. Sin. 33 (7), 2200—2211, (in Chinese with English abstract).

Zhang, X., Zhang, J.P., Huang, X.P., Huang, L.M., 2014. Phytoplankton assemblage structure shaped by key environmental variables in the Pearl River Estuary, South China. J. Ocean Univ. China 13 (1), 1—10.

Zhao, H., 1990. Evolution of the Pearl River Estuary. Ocean Press, Beijing, (in Chinese).